УДК 621.318.24 PACS 07.55.-w; 41.85.Lc

MAGNETIC FIELD CALCULATIONS FOR UNIFORMLY MAGNETIZED BODIES BY THE METHODS OF EQUIVALENT SOLENOIDS AND MAGNETIC CHARGES

M. S. Kustov [a], D. V. Druina [b], O. O. Mikhailova [b], I. G. Polyakov [b], S. E. Ilyashenko [c], R. M. Grechishkin [b]

[a] Insitut Néel, CNRS-UJF, 25 rue des Martyrs, 38042 Grenoble, France
[b] Tver State University, *Laboratory of Magnetoelectronics*
[c] Tver State Technical University, *Chair of metal technology and materials science*

A derivation of analytical formulas for uniformly magnetized bodies of simple is given making use of the formalisms of equivalent surface currents or surface magnetic charges. In contrast to the textbook solutions confined to some points of symmetry, the general results are given for an arbitrary off-axis point of observation. Computer combination of the obtained formulas by the principle of superposition gives an efficient way to examine a large number of practically important cases, including multipole distributions, Halbach configurations, magnetic bearings, levitation systems, etc.
Keywords: *magnetic field calculations, superposition principle, Bio-Savart and Coulomb law, equivalent solenoid, magnetic pole formalism*

РАСЧЁТ МАГНИТНЫХ ПОЛЕЙ ОДНОРОДНО НАМАГНИЧЕННЫХ ТЕЛ МЕТОДАМИ ЭКВИВАЛЕНТНОГО СОЛЕНОИДА И МАГНИТНЫХ ЗАРЯДОВ

М. С. Кустов [a], Д. В. Друина [b], О. О. Михайлова [b], И. Г. Поляков [b], С. Е. Ильяшенко [c], Р. М. Гречишкин [b]

[a] Insitut Néel, CNRS-UJF, 25 rue des Martyrs, 38042 Grenoble, France
[b] Тверской государственный университет, *лаборатория магнитоэлектроники*
[c] Тверской государственный технический университет, *кафедра технологии металлов и материаловедения*

Даны выводы аналитических формул для внешнего магнитного поля однородно намагниченных тел простых форм с использованием формализмов эквивалентного соленоида и поверхностных магнитных зарядов. В отличие от приводимых в учебниках решений, ограниченных отдельными точками симметрии, выводы сделаны для произвольных внеосевых точек наблюдения. Компьютерное комбинирование по принципу суперпозиции позволяет исследовать многие практически ценные случаи, включая мультипольные распределения, конфигурации Хальбаха, магнитные подшипники, системы левитации и др.
Ключевые слова: *расчёт магнитного поля, принцип суперпозиции, закон Био-Савара и Кулона, эквивалентный соленоид, магнитные заряды*

Introduction. High-coercivity permanent magnets are widely used in numerous types of devices. Field calculation of permanent magnets has been approached in a number of different ways, and over the years many authors have published sophisticated computer programs and solutions to a large number of problems. In the present work we offer derivations based only on the most fundamental laws (those of Biot-Savart and Coulomb) and numerical integration. As will be seen, the solutions may be simple but cover many practical cases.

In modern high-coercive rare-earth permanent magnets the residual magnetization vector, $\mu_0 M_r$, is strongly fixed to the easy axis of magnetization. Consequently the magnetization remains uniform even in the presence of rather large demagnetizing fields. This rigidity of magnetization radically simplifies the computation of the fields produced by the magnets and justifies the application of superposition principles for systems composed of many elements.

In fact, rare-earth magnets are nearly ideal models of uniformly magnetized bodies as represented by surface Amperian currents [2] forming an equivalent solenoid. Thereby Biot-Savart law is applicable to the calculation of the field of such a body.

This point needs some discussion, because the same body may be alternatively represented by magnetic poles (charged surfaces). In most modern textbooks on electricity and magnetism (see e.g. [3]) the current-current forces, conduction or Amperian, are taken as fundamental, thus giving the subject a unity not attained by the older magnetic pole concept. However, as was pointed out by W.F. Brown [4], this unity is an illusion in several respects, one of which is that the interpretation of an electron spin moment as an Amperian current has no surer basis than its interpretation as a pair of poles. Although it has been criticized from a pedagogical point of view [5], the use of magnetic poles in analogy to electrostatics is firmly established in research articles and books on ferromagnetism. The problem of reconciling of the two interpretations has been discussed in detail [4]. In the following both approaches are considered to be of equal standing and their application will be demonstrated in parallel.

II. BASIC RELATIONS. To avoid ambiguity below we write the basic relations (in SI units) as they will be used in this paper.

The magnetic field due to a linear current element $I\mathrm{d}\mathbf{l}$ at a distance $\mathbf{R}$ from it is given by the Biot-Savart law

$$d\mathbf{B} = \frac{\mu_0 I}{4\pi} \frac{[d\mathbf{l} \times \mathbf{R}]}{R^3}. \qquad (1)$$

Assuming that the total flux density (magnetic induction) in the magnetized medium is given by

$$\mathbf{B} = \mu_0(\mathbf{H} + \mathbf{M}), \tag{2}$$

the direction of the vector of equivalent current density $\mathbf{I}_m$ (in A m^{-1}) at the media interface will be defined by the cross product

$$\mathbf{I}_m = [\mathbf{M}_1 - \mathbf{M}_2] \times \mathbf{n}, \tag{3}$$

where $\mathbf{n}$ is the normal directed from the medium with magnetization $\mathbf{M}_1$ toward medium with $\mathbf{M}_2$ ($\mathbf{M}_2 = 0$ in vacuo).

Defining the magnetic pole strength (magnetic charge) m_1 (in webers) from the Coulomb law

$$\mathbf{F} = \frac{m_1 m_2}{4\pi\mu_0 R^3}\mathbf{R} \tag{4}$$

the magnetic fieldstrength due to magnetic charges uniformly distributed over a surface element dS will be written as

$$d\mathbf{H} = \frac{\sigma dS}{4\pi\mu_0}\frac{\mathbf{R}}{R^3} \tag{5}$$

where σ is the surface charge density given by the dot product

$$\sigma = \mu_0(\mathbf{M}_1 - \mathbf{M}_2)\mathbf{n}. \tag{6}$$

In a permanent magnet the residual magnetization, $\mu_0\mathbf{M}_r$, is by definition equal to the residual induction (remanence), $\mathbf{B}_r$. The latter parameter commonly serves to characterize permanent magnet materials and will be used in this paper.

III. AXISYMMETRICAL BODIES

A. Circular turn and thin walled solenoid

The magnetic field of a circular turn has been recently considered in detail by Erlichson [1] and for the sake of completeness will be outlined here. Fig. 1 shows the geometry of the problem. From symmetry, the B_y component at the point of observation $P(x_0, y_0, z_0)$ has to be zero, so the problem reduces to the determination of B_x and B_z.

In the coordinate form the cross product [d$\mathbf{l} \times \mathbf{R}$] is given in an obvious notation by

$$[d\mathbf{l} \times \mathbf{R}] = \mathbf{i}\begin{vmatrix} dl_y & dl_z \\ R_y & R_z \end{vmatrix} - \mathbf{j}\begin{vmatrix} dl_x & dl_z \\ R_x & R_z \end{vmatrix} + \mathbf{k}\begin{vmatrix} dl_x & dl_y \\ R_x & R_y \end{vmatrix}, \tag{7}$$

whereas $R^2 = z_0^2 + x_0^2 + a^2 - 2ax_0\cos\varphi$. Applying the Biot-Savart law and choosing appropriate expressions for d**l** and **R** projections we find

$$B_x = \frac{\mu_0 I}{4\pi}\int_0^{2\pi}\frac{dl_y R_z - dl_z R_y}{R^3}$$

$$= \frac{\mu_0 I}{4\pi}\int_0^{2\pi}\frac{az_0\cos\varphi d\varphi}{\left(z_0^2 + x_0^2 + a^2 - 2ax_0\cos\varphi\right)^{3/2}}, \qquad (8)$$

$$B_z = \frac{\mu_o I}{4\pi}\int_0^{2\pi}\frac{dl_x R_y - dl_y R_x}{R^3} = \frac{\mu_o I}{4\pi}\int_0^{2\pi}\frac{a(a - x_o\cos\varphi)d\varphi}{\left[z_o^2 + x_o^2 + a^2 - 2ax_o\cos\varphi\right]^{3/2}} \qquad (9)$$

which apart from some difference in notation coincide with the results of Erlichson [1].

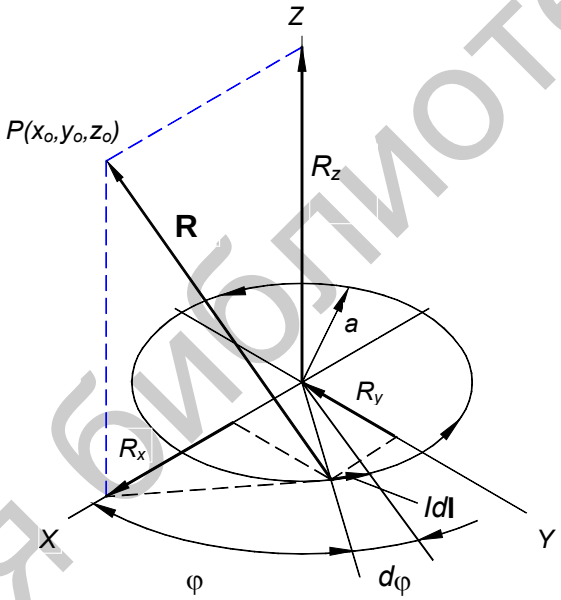

Fig. 1. Diagram for the circular turn. *Id***l** is the linear current element

In proceeding further to the case of a thin-walled solenoid (8) and (9) should be integrated over the solenoid length 2*h*. Taking into account that the current of an elementary ring of a height *dz* is *Idz*/2*h* one obtains

$$B_x = \frac{\mu_0}{4\pi}\frac{I}{2h}\int_{-h}^{h}\int_0^{2\pi}\frac{a(z_0 - z)\cos\varphi d\varphi dz}{\left[(z_0 - z)^2 + x_0^2 + a^2 - 2ax_0\cos\varphi\right]^{3/2}} \qquad (10)$$

$$B_z = \frac{\mu_o}{4\pi}\frac{I}{2h}\int_{-h}^{h}\int_{0}^{2\pi}\frac{a(a - x_o\cos\varphi)d\varphi dz}{\left[(z_o - z)^2 + x_o^2 + a^2 - 2ax_o\cos\varphi\right]^{3/2}}. \qquad (11)$$

Making use of a subsidiary variable $u = z_0 - z\left(du = -dz\right)$ one finds that the integrands in u are of the form $uU^{-3/2}$ and $U^{-3/2}$, where $U = Au^2 + Bu + C$ (A, B, C constants). The corresponding integrals are expressed in terms of elementary functions [6]. With this provision (10) and (11) reduce to

$$B_x = \frac{2\mu_o a}{4\pi}\frac{I}{2h}\int_{o}^{\pi}\left\{\frac{\cos\varphi d\varphi}{\left[(z_o - z)^2 + x_o^2 + a^2 - 2ax_o\cos\varphi\right]^{1/2}}\right\}_{z=-h}^{z=h} \qquad (12)$$

$$B_z = \frac{2\mu_o a}{4\pi}\frac{I}{2h}\int_{o}^{\pi}\left\{\frac{(z_o - z)(a - x_o\cos\varphi)d\varphi}{\left[(z_o - z)^2 + x_o^2 + a^2 - 2ax_o\cos\varphi\right]^{1/2}}\right\}_{z=-h}^{z=h}$$

$$\times\left\{\frac{(z_0 - z)}{\left[(z_0 - z)^2 + x_0^2 + a^2 - 2ax_0\cos\varphi\right]^{1/2}}\right\}_{z=-h}^{z=h} \qquad (13)$$

Eqs. (12) and (13), as well as (8) and (9) (circular turn) could be expressed in terms of complete elliptic integrals of the first and second kind. However, following the arguments of Erlichson [1], we recommend here the numerical solution of these equations by any decent numerical integration routine.

B. Disk of uniform pole density (Fig. 2)

Making use of (5) and taking into account that the surface element $dS = rdrd\varphi$ one arrives at integrals

$$B_x = \frac{\sigma}{4\pi}\int_{r=o}^{r=a}\int_{o}^{2\pi}\frac{(x_o - r\cos\varphi)rdrd\varphi}{\left[z_o^2 + x_o^2 + r^2 - 2rx_o\cos\varphi\right]^{3/2}}$$

$$= \frac{\sigma}{4\pi}\int_{o}^{2\pi}\left[\frac{(4C - 2B^2)r - 2BC}{(B^2 - 4C)U^{1/2}} + \ln\left|2U^{1/2} + 2r + B\right|\right]_{r=o}^{r=a}\cos\varphi d\varphi$$

$$= \frac{2\sigma}{4\pi}\int_0^{\pi}\left\{\frac{x_0(2Br+4C)-\cos\varphi\left[(4C-2B^2)r-2BC\right]}{(B^2-4C)U^{1/2}}\right.$$

$$\left.-\cos\varphi\ln\left|2U^{1/2}+2r+B\right|\right\}_{r=0}^{r=a} d\varphi\,. \qquad (14)$$

$$Bz = \frac{\sigma}{4\pi}\int_{r=0}^{r=a}\int_0^{2\pi}\frac{z_0 r dr d\varphi}{\left[z_0^2+x_0^2+r^2-2rx_0\cos\varphi\right]^{3/2}}$$

$$= \frac{\sigma z_0}{4\pi}\int_0^{2\pi}\left[\frac{2Br+4C}{(B^2-4C)U^{1/2}}\right]_{r=0}^{r=a} d\varphi \qquad (15)$$

where $B=-2x_0\cos\varphi$, $C=x_0^2+z_0^2$, and $U=r^2+Br+C$.

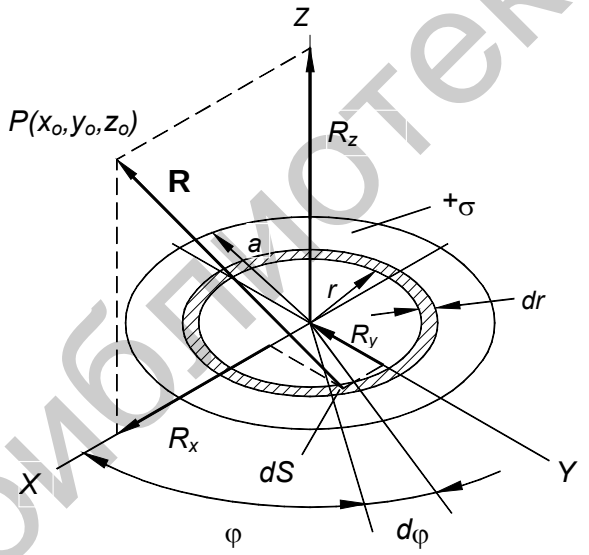

F i g . 2. Diagram for the uniformly charged disk. $dS = rdrd\varphi$ is a surface element

As above in this case it was possible to express external integrals over r in (14) and (15) in terms of elementary functions while the resulting expressions should be integrated numerically.

It is worthwhile to mention that Eqs. (14) and (15) derived for a single charged disk have meaning only as a one module of a sum over all positively and negatively charged surfaces constituting the real sample.

C. Axially magnetized cylinders and rings (Figs. 3, a; b)

Eqs. (12) and (13) (thin-walled solenoid) as well as (14) and (15) (charged disk) provide the basis for calculations of B_x and B_y field components of axially magnetized axisymmetrical bodies at any observation point.

As to the current model, (12) and (13) may be immediately used for permanent magnet field calculations when the coefficient $\mu_0 I/2h$ outside the integral sign is replaced by B_r, permanent magnet remanence.

For the equivalent charge model (Eqs. (14) and (15)) the axially magnetized cylinder should be represented by a pair of oppositely charged disks at a distance $2h$ apart from each other with their fields beeing superimposed for each point of observation. In doing so the coefficient σ should be replaced by B_r.

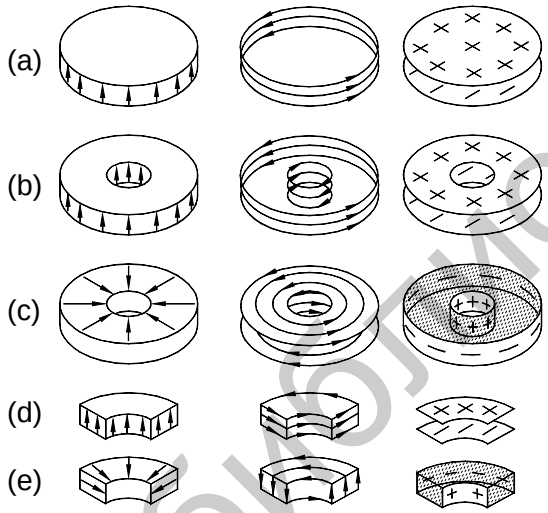

Fig. 3. Presentation of axisymmetrical magnets (left column) by Amperian currents (middle column) and surface charges (right column). (a) – axially magnetized disk, (b) – axially magnetized ring, (c) – radially magnetized ring, (d), (e) – axially and radially magnetized ring segments, respectively. Hatching indicates the existence of volume charges in two specific cases of radial magnetization

In Figs. 3, *a* and *b* the current and charge presentation is sketched for axially magnetized cylinders and rings. For the former case the ring is represented by two superimposed oppositely magnetized cylinders of equal height and diameters equal to the outer and inner ring diameter, respectively. For the charge model the solution is obtained just by substitution of $r = a_1$

(inner ring radius) for the lower limit of integration in Eqs. (14) and (15), while the upper limit $r = a_2$ should be standing for the outer ring radius.

D. Radially magnetized rings

The presentation of a ring with radial magnetization frequently used in microwave devices is illustrated in Fig. 3, *c* for both models.

In the current model such a ring is represented by two flat spiral solenoids. The calculation is much the same as above with the difference that now the integration of the field of a current ring is performed in the radial direction.

For example, the B_z component of a single flat spiral solenoid will be given by

$$\begin{aligned} B_z &= \frac{\mu_o}{4\pi}\frac{I}{a_2-a_1}\int_{a_1}^{a_2} da \int_0^{2\pi} \frac{a(a-x_o\cos\varphi)d\varphi}{\left[a^2-2ax\cos\varphi+x_o+z_o^2\right]^{3/2}} \\ &= \frac{\mu_o}{4\pi}\frac{I}{a_2-a_1}\int_o^{2\pi}\{\frac{a}{a^2-2ax_o\cos\varphi+x_o^2+z_o^2} \\ &\quad +\ln\left|a-x_o\cos\varphi+\sqrt{a^2-2ax_o\cos\varphi+x_o^2+z_o^2}\right|\}_{a=a_1}^{a=a_2} d\varphi, \end{aligned} \tag{16}$$

where a_1 and a_2 stand for the inner and outer spiral radius, respectively. To obtain the total field of the ring (16) should be used twice for two flat spirals at a distance 2*h* apart. In doing so the change of the current direction for the two solenoids should be accounted for as illustrated in Fig. 3, *c*.

To obtain the similar result by the charge model it is necessary to take into account *volume* charges arising inside the ring, because for this specific case the uniformity of magnetization is violated due to its radial character. Evidently this requires additional calculational efforts not encountered in the current model and so will not be considered here.

In addition to the cases considered above Figs. 3, *d* and *e* illustrate the presentation of ring segments, magnetized axially or radially, by both models. Such segments are widely used in modern brushless motors. It is seen that their field may be calculated equally well by the methods described provided appropriate limits of integration corresponding to the radial and angular segment dimensions are used and the contribution of the lateral cross-sectional segment sides is taken into account.

IV. TETRAGONAL PRISMS

A. Rectangular current turn and thin solenoid (Fig. 4).

From the Biot-Savart law (1) and the cross-product expression (7) it follows that

$$dB_x = \frac{\mu_o I}{4\pi R^3} dl_y R_z, \qquad dB_y = \frac{\mu_o I}{4\pi R^3} dl_x R_z,$$

$$dB_z = \frac{\mu_o I}{4\pi R^3} (dl_x R_y - dl_y R_x), \tag{17}$$

while $R^2 = (x_0 - x)^2 + (y_0 - y)^2 + (z_0 - z)^2$.

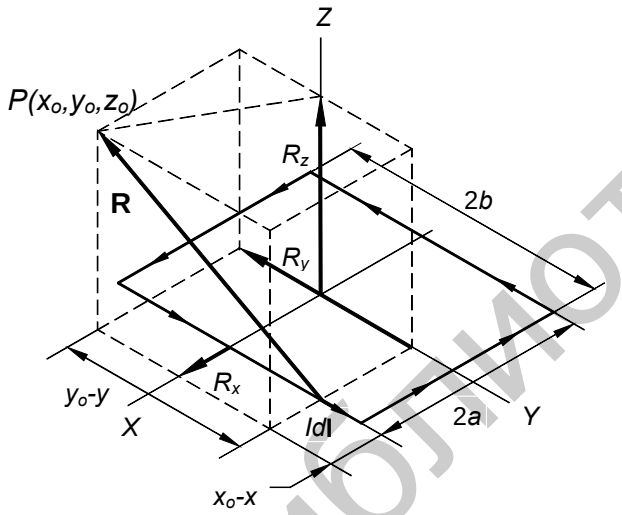

Fig. 4. Diagram for the rectangular current turn

Integrating (17) over the sides of the turn from -*a* to *a* and -*b* to *b* followed by integration over the height 2*h* of a thin solenoid based on this turn one obtains simple expressions in terms of elementary functions as follows:

$$dB_x = -\frac{\mu_o}{4\pi}\frac{I}{2h}\left[\left(\int_{-h}^{h} \frac{\beta(z_o - z)dz}{\left[\alpha^2 + (z_o - z)^2\right]\sqrt{\alpha^2 + \beta^2 + (z_o - z)2}}\right)_{\alpha_1}^{\alpha_2}\right]_{\beta_1}^{\beta_2} \tag{18}$$

$$= -\frac{\mu_o}{4\pi}\frac{I}{2h}\left\{\left[\left(\ln\left(\beta + \sqrt{\alpha^2 + \beta^2 + \gamma^2}\right)\right)_{\alpha_1}^{\alpha_2}\right]_{\beta_1}^{\beta_2}\right\}_{\gamma_1}^{\gamma_2},$$

$$B_y = -\frac{\mu_o}{4\pi}\frac{I}{2h}\left\{\left[\left(\ln\left(\alpha+\sqrt{\alpha^2+\beta^2+\gamma^2}\right)\right)_{\alpha_1}^{\alpha_2}\right]_{\beta_1}^{\beta_2}\right\}_{\gamma_1}^{\gamma_2}, \qquad (19)$$

$$B_z = -\frac{\mu_o}{4\pi}\frac{I}{2h}[(\int_{-h}^{h}\frac{\alpha\beta dz}{[\beta^2+(z_o-z)^2]\sqrt{\alpha^2+\beta^2+(z_0-z)^2}} + \int_{-h}^{h}\frac{\alpha\beta dz}{[\alpha^2+(z_o-z)^2]\sqrt{\alpha^2+\beta^2+(z_0-z)^2}})_{\alpha_1}^{\alpha_2}]_{\beta_1}^{\beta_2} \qquad (20)$$

$$= -\frac{\mu_o}{4\pi}\frac{I}{2h}\left\{\left[\left(\tan^{-1}\frac{\gamma+\sqrt{\alpha^2+\beta^2+\gamma^2}}{\alpha\beta}\right)_{\alpha_1}^{\alpha_2}\right]_{\beta_1}^{\beta_2}\right\}_{\gamma_1}^{\gamma_2},$$

where α, β and γ are standing for the limits of definite integrals implying that

$$\left\{\left[f(\alpha,\beta,\gamma)_{\alpha_1}^{\alpha_2}\right]_{\beta_1}^{\beta_2}\right\}_{\gamma_1}^{\gamma_2} = f(\alpha_2\beta_2\gamma_2) - f(\alpha_1\beta_2\gamma_2) - f(\alpha_2\beta_1\gamma_2)$$
$$+ f(\alpha_1\beta_1\gamma_2) - f(\alpha_2\beta_2\gamma_1) + f(\alpha_1\beta_2\gamma_1) + f(\alpha_2\beta_1\gamma_1) - f(\alpha_1\beta_1\gamma_1),$$

where $\alpha_{1,2} = x \pm a, \beta_{1,2} = y_o \pm b, z_{1,2} = z \pm h$ (+ and − signs apply to subscripts 1 and 2, respectively).

Fortunately, it was possible to perform triple integration in the above derivation in closed form, hence the expressions (18) - (20) are exact [7].

According to the Coulomb law (5) the magnetic fieldstrength of a surface element $dS = dxdy$ is

$$d\mathbf{B} = \sigma dxdy\frac{\mathbf{R}}{R^3}$$

Integration over the sides of the sheet from -a to a and -b to b yields

$$B_x = \frac{\sigma}{4\pi}\left\{\left[\ln\left(\beta+\sqrt{\alpha^2+\beta^2+(z_o-z)^2}\right)\right]_{\alpha_1}^{\alpha_2}\right\}_{\beta_1}^{\beta_2}, \qquad (21)$$

$$B_y = \frac{\sigma}{4\pi}\left\{\left[\ln\left(\alpha + \sqrt{\alpha^2 + \beta^2 + (z_o - z)^2}\right)\right]_{\alpha_1}^{\alpha_2}\right\}_{\beta_1}^{\beta_2}, \qquad (22)$$

B. Rectangular sheet of uniform pole density (Fig. 5)

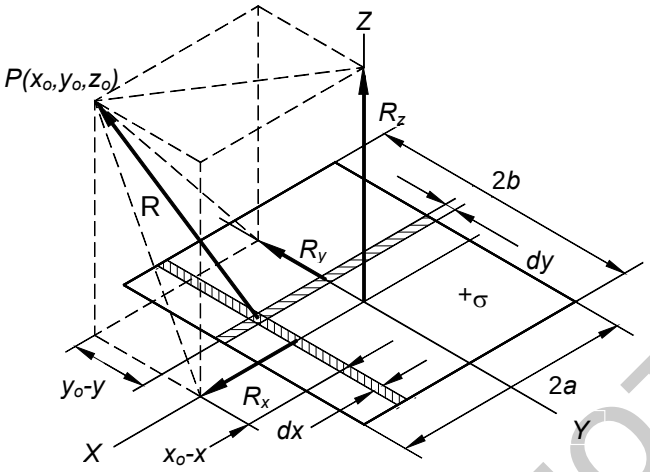

Fig. 5. Diagram for the rectangular sheet of uniform pole density $+\sigma$

$$B_z = \frac{\sigma}{4\pi}\left\{\left[\tan^{-1}\frac{\alpha\beta}{\gamma\sqrt{\alpha^2 + \beta^2 + (z_o - z)^2}}\right]_{\alpha_1}^{\alpha_2}\right\}_{\beta_1}^{\beta_2}, \qquad (23)$$

where $\alpha_{1,2}$ and $\beta_{1,2}$ have the same meaning as above.

C. Tetragonal prismatic magnet: axial and inclined magnetization

A scheme representing the axially magnetized tetragonal prisms by currents or charges is given in Fig. 6, *a*.

The interpretation is similar to cylinders shown in Fig. 3, *a*, namely rectangular solenoid formulas (18-20) are ready for use immediately after replacing $\mu_0 I/2h$ by the remanence B_r, while for the charge model a superposition of the field from two distant oppositely charged sheets should be performed with replacing surface charge density σ by B_r in formulas (21)-

(23). With this provision (21) and (22) (B_x and B_y components) get exactly the same form as (18) and (19) (current model), while B_z is expressed as

$$B_z = \frac{B_r}{4\pi}\left\{\left[\tan^{-1}\frac{\alpha\beta}{\gamma\sqrt{\alpha^2+\beta^2+\gamma^2}}\right]_{\alpha_1}^{\alpha_2}\right\}_{\beta_1}^{\beta_2}. \qquad (24)$$

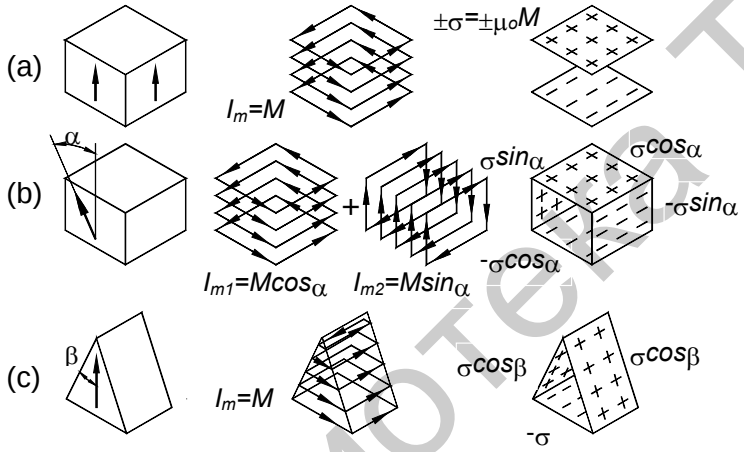

Fig. 6. Presentation of prismatic magnets (left column) by Amperian currents (middle column) and surface charges (right column). See comments in the text

Both models appear to be universal enough to describe a rather special case of magnetization inclined with respect to the prism edges. A specific case of **M** rotation by an angle φ in the *ZY* plane is illustrated in Fig. 6, *b*. Two superimposed solenoids with orthogonal magnetization directions appear to be adequate for the description of this case provided appropriate magnetization values are ascribed to each of them, while four charged sheets should be used to this end with the charge model. In the general case of φ arbitrary (not shown in the figure) three superimposed solenoids or six charged sheets are needed.

Still another application of the models to triangular prisms is depicted in Fig. 6, *c*. Such triangular prisms are effective as building blocks in some modern permanent magnet systems [8-9].

Fig. 7 shows how the magnetization orientation in two adjacent rectangular blocks affects the total B_z field at some distance above the

magnets. It is seen that B_Z passes through a maximum with the change of abs(φ) from zero to π/2. A three-fold increase in the peak value of B_Z is observed when $\varphi_{\cdot} \cong 70^{o}$ thus demonstrating the performance improvement obtainable in the so-called convergent magnet structure [10].

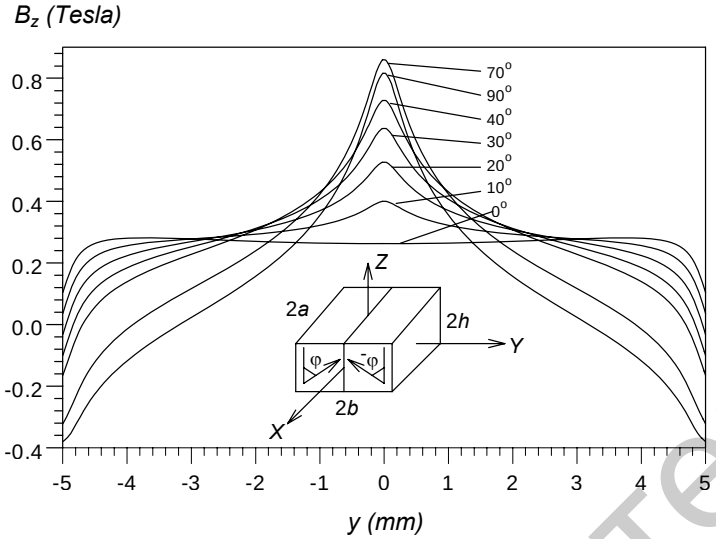

Fig. 7. Variation of the B_z field near the upper surface (δ = 0.2 mm) of a convergent magnet structure as dependent on the orientation of magnetization in adjacent blocks. For φ = 0 the system behaves like a single magnet, otherwise a maximum in B_z occurs. $2a$ = 15, $2b$ = 10, $2h$ = 5 mm, B_r = 0.9 T.

V. DISCUSSION AND CONCLUSION

The above given derivations show that both current and charge models may be in principle equally well employed to the description of various permanent magnet configurations. Some advantages may be found in a particular model from the mathematical point of view or when keeping up the tradition is desirable. For example, the current model requires simpler mathematics when axisymmetrical bodies are considered. On the other hand we find the charge model more convenient in the analysis of complex polygonal shapes. Also the charge model is by tradition almost exclusively employed in a such well-developed field of research as magnetic domain theory [11-13].

Juxtaposing the two models provides a very instructive insight into the problem of external and internal field of magnetized bodies. To illustrate this important matter in Fig. 8 we present the field distribution for a cubic

sample (magnetized along the *Z*-direction) as obtained by two methods [Eqs. (20) and (24)].

The external field is exactly the same for both presentations, whereas inside the sample only B_X field components coincide with each other. As to the B_Z components they differ inside the sample exactly by the value of $\mu_0\mathbf{M}$, in full accordance with basic relation (2). In other words, the current model gives the **B** value everywhere, while it is the subsidiary vector quantity $\mu_0\mathbf{H}$ that is given by the charge model [14]. At the same time B_X and B_Y remain the same for both approaches because for this particular case $\mu_0 M_X = \mu_0 M_Y = 0$. This arguments explain why the formulas for B_X and B_Y are the same when different models are applied to tetragonal prisms. In contrast, similar pair of formulas (12) and (14) (cylinders) are of markedly different appearance. We were not able to bring them into the same form analytically. However, the numerical check confirmed their full consistency with the above deduction within the error of integration.

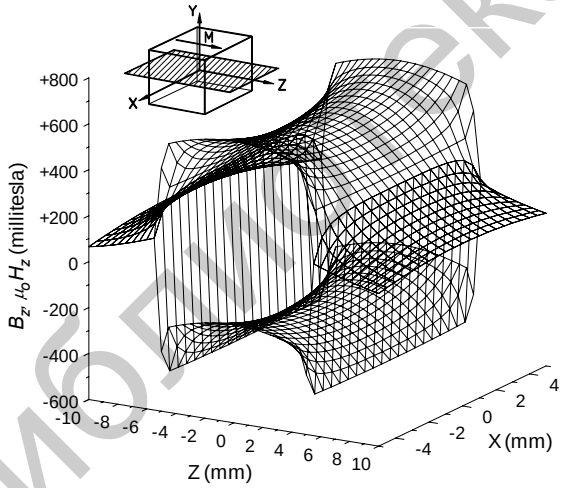

Fig. 8. Magnetic induction B_z and field intensity $\mu_0 H_z$ in the central *XZ* plane for a 10×10×10 mm *Z*-magnetized cube as calculated by equivalent current (upper graph) and charge (lower graph) formalisms. The values are the same outside the body and differ exactly by $\mu_0 M_z = B_r = 0.8$ T ($M_x = M_y = 0$) inside it. Dashed surface in the inset indicates the observation plane

The inside $\mu_0\mathbf{H}$ derived by any model (to obtain $\mu_0\mathbf{H}$ inside the sample by the current model just subtract $\mu_0\mathbf{M}$ from **B**) is in fact the so-called self-demagnetizing field. It is worthwhile to recall that in non-ellipsodal bodies the demagnetizing field is not uniform [15]. This fact is generally accounted for by introducing a ballistic (averaged over the central cross-section) and magnetometric (averaged over the whole sample volume) demagnetizing factors [26]. These may be computed provided $\tilde{\mu_0}\mathbf{H}$ is

characterized locally inside the sample. In this way we were able to reproduce exactly the known tables of demagnetizing factors for cylinders and rectangular prisms derived otherwise in a more complex fashion. Evidently other magnet shapes may be characterized in the same way.

Still another application of the results presented is connected to the calculation of both external and internal fields arising from magnetic domains. To this end we may think of a magnetic domain as a permanent magnet. This is justified because generally the domain wall thickness is small compared to the domain size. With this provision the above derivations may be directly applied to a variety of magnetic domain structures. An illustration of this approach to the analysis of some typical domain structures is given in Fig. 9.

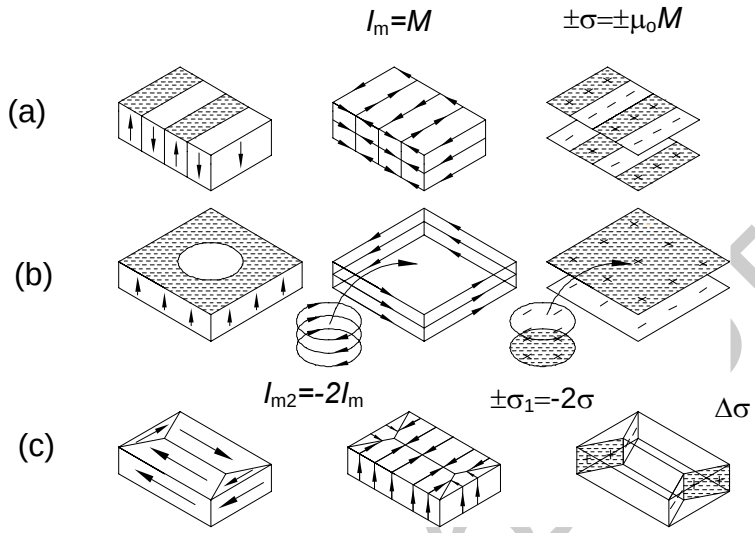

Fig. 9. Presentation of some typical domain structures (DS) by Amperian currents and magnetic charges. (a) Kittel-type stripe 180° DS, (b) cylindrical (bubble) DS, (c) closed 90° DS in a crystal having cubic anisotropy

The final remark completing the discussion is that the results given also may be applied to the calculation of permanent magnet systems including magnetically soft elements, e.g. back iron. In doing so the method of images well known in electrostatics [3] may be succesfully exploited assuming infinite magnetic permeability of the backing elements. With this provision the problem reduces to that of summing up the contribution of a series of regularly positioned images of the main magnet by the same formula. The sum of the first n terms of such a series differs numerically from the total sum by less than the absolute value of the (n+1)-th term. Usually n of the order of 5-10 is sufficient to obtain adequate accuracy in good accordance with experiment.

In conclusion, we have demonstrated that straightforward calculations of a variety of permanent magnet configurations is feasible from the first principles given by the fundamental laws supported by simple numerical techniques. The calculational details presented have not previuosly been available in a single paper.

The results of this study may be used either at the introductory courses in electromagnetism or at advanced level of training, appealing to students who, while lacking experience in more sophisticated aspects of magnetic field calculations, find the more elementary approach unsatisfactory.

Acknowledgements

The authors gratefully acknowledge the RTRA Fondation Nanosciences and Federal Target Program "Research and Research_Pedagogical Personnel of Innovation Russia for 2009–2013" for the support of this work.

Appendix

For ready reference the above derived general formulas are written below for particular cases of the B_z field component on the magnet Z-axis, as a function of coordinate z_0, when the solutions are greatly simplified.

Circular turn of radius a:

$$B_z^{x=y=0}(z_0)=\frac{\mu_0 I}{2}\frac{a^2}{\left(a^2+z_0^2\right)^{3/2}}\ .$$

Charged disk of radius a:

$$\mu_0 H_z^{x=y=0}(z_0)=\frac{\sigma}{2}\left(1-\frac{z_o}{\left(a^2+z_0^2\right)^{1/2}}\right).$$

Axially magnetized cylinder of height 2h:

$$B_z^{x=y=0}(z_0)=\frac{B_r}{2}\left\{\frac{\gamma}{\left(a^2+\gamma^2\right)^{1/2}}\right\}_{\gamma_1=z_0+h}^{\gamma_2=z_0-h}\ .$$

Axially magnetized ring:

$$B_z^{x=y=0}(z_0)=\frac{B_r}{2}\left\{\left[\frac{\gamma}{\left(a^2+\gamma^2\right)^{1/2}}\right]_{a_1}^{a_2}\right\}_{\gamma_1=z_0+h}^{\gamma_2=z_0-h}\ .$$

where a_1 = inner, a_2 = outer ring radius.

Flat spiral solenoid:

$$B_z^{x=y=0}(z_0) = \frac{\mu_0}{2}\frac{NI}{a_2 - a_1}$$

$$\times\left[-\frac{a}{\left(a^2+\gamma^2\right)^{1/2}} + \ln\left(a+\sqrt{a^2+\gamma^2}\right)\right]_{a_1}^{a_2},$$

where N = number of turns.

Radially magnetized ring:

$$B_z^{x=y=0}(z_0) = \frac{B_r}{2}\left[\left(\frac{1}{\xi_1}-\frac{1}{\xi_2}\right)-\left(\frac{1}{\zeta_1}-\frac{1}{\zeta_2}\right)+\ln\left|\frac{(1+\zeta_1)(1+\xi_2)}{(1+\zeta_2)(1+\xi_1)}\right|\right],$$

$$\xi_{1,2} = \frac{\left[a_1^2+(h\mp z_0)^2\right]^{1/2}}{a_1}, \quad \zeta_{1,2} = \frac{\left[a_2^2+(h\mp z_0)^2\right]^{1/2}}{a_2},$$

where - and + signs apply to subscripts 1 and 2, respectively.

Rectangular current turn 2a × 2b:

$$B_z^{x=y=0}(z_0) = \frac{\mu_0 I}{\pi}\frac{ab}{\left(a^2+b^2+z_0^2\right)^{1/2}}\left(\frac{1}{b^2+z_0^2}+\frac{1}{a^2+z_0^2}\right).$$

Rectangular charged sheet 2a × 2b:

$$\mu_0 H_z^{x=y=0}(z_0) = \frac{\sigma}{\pi}\tan^{-1}\frac{ab}{z_0\sqrt{a^2+b^2+z_0^2}}.$$

Tetragonal prism 2a × 2b × 2h:

$$B_z^{x=y=0}(z_0) = -\frac{B_r}{\pi}\left[\tan^{-1}\frac{\gamma\sqrt{a^2+b^2+\gamma^2}}{ab}\right]_{\gamma_1=z_0+h}^{\gamma_2=z_0-h},$$

$$\mu_0 H_z^{x=y=0}(z_0) = \frac{B_r}{\pi}\left[\tan^{-1}\frac{ab}{\gamma\sqrt{a^2+b^2+\gamma^2}}\right]_{\gamma_1=z_0+h}^{\gamma_2=z_0-h}.$$

Part of these formulas may be found in standard texbooks on electromagnetism. However, here they arrive from the simplification of

corresponding general equations rather than from direct elementary derivation.

References

1. Erlichson H. The magnetic field of a circular turn //Am. J. Phys. 1989. V. 57. P.607–610.
2. The illustration of magnetized *cylinder* with molecular currents cancelling each other inside the body and leaving uncompensated surface current is recuring in textbooks perhaps from the times of Ampere. But for the *cylinder* in contrast to the *ellipsoid* it is hardly at all to expect that this presentation has been ever justified experimentally before the invention of high-coercivity materials, because older types of permanent magnets are characterized by $\mu_0 H_C < \mu_0 M_r$, hence in an open magnetic circuit the cylinder self-demagnetizing field disturbs the magnetization thus giving rise to *volume* currents in addition to surface ones.
3. Feynman R. P., Leighton R. B., Sands M. The Feynman Lectures on Physics // Addison Wesley, Reading, MA. 1964. V. II (имеется русский перевод: Фейнман Р., Лейтон Р., Сэндс М. Фейнмановские лекции по физике. Том 5: Электричество и магнетизм. Перевод с английского (издание 3).
4. Brown W. F. Magnetostatic Principles in Ferromagnetism // North-Holland Publ.Co. Amsterdam. 1962.
5. Warburton F. W. The magnetic pole, a useless concept //Am. Phys. Teacher (Am. J. Phys.). 1934. V. 2. P. 1–6.
6. Dwight H. B., Tables of integrals (MacMillan, New York, 1961) (имеется русский перевод: Двайт Г.Б. Таблицы интегралов и другие математические формулы. М.: Наука, 1977).
7. summation formula $\tan^{-1}x - \tan^{-1}y = \tan^{-1}[(x-y)/(1+xy)]$ ($x>0$, $y>0$) is helpful when folding the final expression (20) for B_z.
8. Leupold H. A., Tilak A. S., Potenziani E. II, Tapered fields in cylindrical and spherical spaces // IEEE Trans. Magn. 1992. V. 28. P. 3045–3047.
9. Abele M. G. Linear theory of yokeless permanent magnets // J. Magn. Magn. Mater. 1990. V. 83. P. 276–278.
10. Blazek Z., Landa V., Novak P. Permanent magnets with convergent anisotropic structure // J. Phys. 1985. V. 46. P. C. 295–C298.
11. Kooy C., Enz U. Experimental and theoretical study of the domain configuration in thin layers of $BaFe_{12}O_{19}$ // Philips Res. Reports. 1960. V. 15. P. 7-29.
12. Hubert A., Schafer R. Magnetic Domains, Springer, Berlin, 1998.
13. O'Handley R.C. Modern Magnetic Materials Principles and Applications. Wiley Interscience, 1999.

14. Parcell E. Electricity and Magnetism. // McGraw-Hill. New York. 1965 (имеется русский перевод: Парселл Э. Берклеевский курс лекций: электричество и магнетизм (Том 2). М.: 1965.
15. Joseph R. I., Schlomann E. Demagnetizing field in nonellipsoidal bodies // J. Appl. Phys. 1965. V. 36. P. 1579–1593.

Об авторах:

КУСТОВ Михаил Сергеевич – научный сотрудник института Нееля, Гренобль (Франция);

ДРУИНА Дарья Викторовна – магистрант кафедры прикладной физики ТвГУ, sabiomoon@mail.ru;

МИХАЙЛОВА Ольга Олеговна – магистрант кафедры прикладной физики ТвГУ;

ПОЛЯКОВ Илья Геннадьевич – студент кафедры общей физики ТвГУ;

ИЛЬЯШЕНКО Светлана Евгеньевна – кандидат физ.-мат. наук, доцент кафедры технологии металлов и материаловедения ТГТУ, SvIlyashenko@yandex.ru;

ГРЕЧИШКИН Ростислав Михайлович – кандидат физ.-мат. наук, профессор кафедры прикладной физики ТвГУ, rmgrech@yandex.ru.